ISSN: 2638-1974

International Journal of Petrochemistry and Research

Research Article

Open Access

The impact of pH and Temperature on Gibbsite reactivity with Quartz

A M. Ali and **Eshwaran Padmanabhan***

Department of Geosciences, Faculty of Geosciences and Petroleum Engineering, Universiti Teknologi Petronas (UTP), 31750, Tronoh, Perak, Malaysia

Article Info

***Corresponding author:**
Eswaran Padmanabhan
Associate Professor
Department of Geosciences
Faculty of Geosciences and Petroleum Engineering
Universiti Teknologi Petronas
31750, Tronoh, Perak, Malaysia
E-mail: eswaran_padmanabhan@utp.edu.my

Received: February 22, 2017
Accepted: April 7, 2017
Published: April 13, 2017

Citation: Ali AM, Padmanabhan E. The impact of pH and Temperature on Gibbsite reactivity with Quartz. *Int J Petrochem Res.* 2017; 1(1): 40-45.
doi: 10.18689/ijpr-1000108

Published by Madridge Publishers

Abstract

In alumina industry, gibbsite ($Al(OH)_3$) precipitation from sodium aluminate solution is the foremost step in the production of alumina (Al_2O_3) from bauxite via the Bayer process. Hence, the precipitation of gibbsite has been extensively studied, with focus on kinetic modelling of the growth and agglomeration of gibbsite under different batch precipitation conditions. However, not much attention has been paid to gibbsite reactivity with quartz, given their ubiquitous nature. Stock solutions containing $AlCl_3$ and quartz grains of varying pH [5.5, 7.5 and 9] were prepared to establish optimum pH conditions for Al-oxides precipitations. The synthesized gibbsite were characterized with FESEM, FTIR and Raman spectroscopy. The competing processes of chemical leaching and dissolution-reprecipitation between quartz and gibbsite showed that gibbsite is distinctly more crystallized with well-defined polygonal structure at higher temperature (60ºC) and low silica. The FESEM micrographs showed that gibbsite can be synthesized in the pH range selected for this study, suggesting gibbsite is synthesizable as long as there are available OH^- ions to hydrolyze $AlCl_3$.

Keywords: Gibbsite; quartz dissolution; surface morphology; FTIR characterization

Introduction

Gibbsite ($Al(OH)_3$) is generally formed from the chemical interactions between weathered rocks and rainwater in hot and humid zones under high rainfall and high leaching rates [1]. The ubiquitous nature of gibbsite in surface formations is generally attributed to the action of high intensity weathering processes for a long duration [2]. This great abundance of gibbsite in soils and weathering products in tropical environments is an indicative factor of advanced stages of weathering that are characteristic of developed soils [3]. Gibbsite is even considered the definitive end product of weathering [4]. Therefore, the study of hydrous gibbsite mineral at variable pressure, pH and temperature conditions is crucial for understanding the dynamic processes and circulation of gibbsite/aluminohydroxides bearing waters [5]. Moreover, gibbsite precipitation from sodium aluminate solution is the foremost step in the production of alumina (Al_2O_3) from bauxite via the Bayer process [6], hence several research has studied gibbsite precipitation with focus on kinetic modeling of the growth and agglomeration of gibbsite under different batch precipitation conditions [7] [8] [9]. However, only a few studies have focused on developing the relationship between gibbsite surface morphology and its growth mechanism [9]. Moreover, related studies do not take into consideration that quartz and Al hydr (oxides) (gibbsite) are principal components of silicaclastics, and the fact that field observations and experimental studies have shown Al oxides form on quartz grains [10] [11].

The reactivity of quartz and gibbsite can act as a control in the growth mechanism of gibbsite. This study is an attempt to elucidate the surficial precipitation and growth mechanism of gibbsite on quartz. Gibbsite reactivity with quartz will either inhibit or catalyze the growth of Al hydr (oxides).This will improve the understanding on the controls of gibbsite solubility. Therefore, the objective of this study is to determine the gibbsite morphology at different pH and temperature conditions as well as to explore the impact of quartz dissolution on gibbsite precipitation.

Materials and Methods

Gibbsite was synthesized on quartz substrates (qAl) by the slow addition of 0.5molL^{-1} KOH to 0.8molL^{-1} $AlCl_3$. Stock solutions of the samples with varying pH [5.5, 7.5 and 9] were prepared. Afterwards, the stock solutions and their replicates were aged for 20days at room temperature (≈25°C) and 60°C. The pH was monitored daily for the 20 days (Fig. 1) to establish optimum pH conditions for Al-hydr (oxide) precipitation. The stock solutions were subsequently drained and the residual substrates dehydrated in an oven set at 40°C for 5 days. The amount of dissolved silica in the drained solution was measured using silica molybdate spectrophotometry method (HACH D2800). Fourier transform infra-red (FTIR) analysis was used to study quartz reactivity with gibbsite by identifying chemical bonds. Morphological variations of the synthesized gibbsite were analyzed using field emission scanning electron microscopy (FESEM). Pure quartz substrate was included in the experiment as a control sample [qAl_0].

Results

pH and quartz dissolution measurements

The daily pH measurements of the stock solutions show that pH declined sharply after 1 day of ageing, as presented in Fig.1. For measurements at pH9 ($qAl_{9(60°C)}$), pH7.5($qAl_{7.5(60°C)}$), and pH5.5 ($qAl_{5.5(60°C)}$) at 60°, the pH decreased sharply to pH4, pH3 and pH3.5, respectively. This decrease is more significant at pH 9. In addition, the decline in pH increases with increasing pH. In contrast, the pH declined less drastically in stock solutions stored at room temperature ($qAl_{5.5}$, $qAl_{7.5}$, qAl_9) from 5.5, 7.5 and 9 to 6.5, 6.5 and 3.5, respectively. Nonetheless, the decline was similarly more significant at pH9. In stock solutions stored at 60°($qAl_{5.5(60°C)}$, $qAl_{7.5(60°C)}$, $qAl_{9(60°C)}$), the pH slightly increased after day 3, and then becomes steady for the remaining days, In contrast, no increase in pH is observed for solutions stored at room temperature.

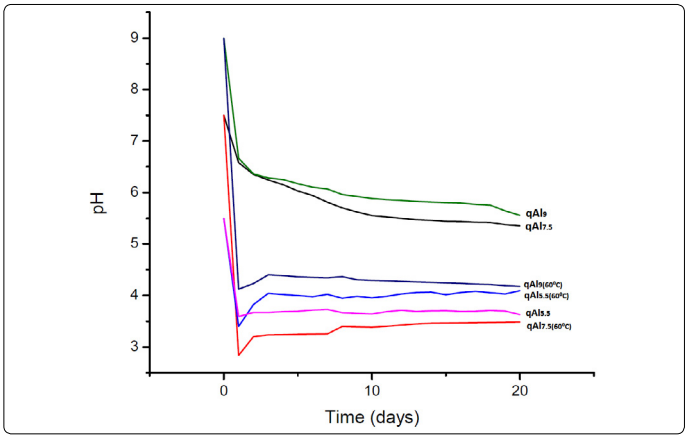

Fig 1. Plot showing variation in pH with time

The amount of dissolved silica was measured for each pH condition, as shown in Table. 1. As observed, the amount of dissolved silica expectedly increased from lower pH to higher pH at room temperature, with values of 9.5, 39.3, and 120 mg/L for $qAl_{5.5}$, $qAl_{7.5}$, and qAl_9, respectively, given that quartz dissolves at low and high pH. At a higher temperature (60°), the dissolved silica in the system increased to as high as 180mg/L at pH 9 (Table. 1).

Table 1. Dissolved silica at different synthesis conditions of gibbsite

Sample	$qAl_{5.5}$	$qAl_{5.5(60°C)}$	$qAl_{7.5}$	$qAl_{7.5(60°C)}$	qAl_9	$qAl_{9(60°C)}$	qAl_0
Dissolved silica [mg/L]	9.5	110.9	39.3	111.5	120	180.4	36.9

FTIR characterization

FTIR spectra was obtained for the different synthesis conditions, as shown in Fig. 2. The FT-IR peaks at approximately 775 and 1080cm^{-1} (Fig.2) denote Si-O quartz bonds, while the peak at 1600cm^{-1} signifiesH-O-H bending of water. Al---O-H stretching bond was absent. O-H stretching modes common to most phyllosilicates lie in the spectral region of 3400 to 3750 cm^{-1}. Metal-OH bending modes occur in the 600 to 950 cm^{-1} region. Si-O and Al-O stretching modes are found in the 700 to 1200 cm^{-1} range. Si-O and Al-O bending modes dominate the 150 to 600 cm^{-1} region. Four bands at 914, 972, 1021 and 1060 cm^{-1} correspond to OH-bending vibrations. Most probably, the lower frequency band at 914 cm^{-1} is attributed to the Al-O-H group with the least hydrogen bonding influence. The bands in the 500 to 650 cm^{-1} region are overlaps of out-of-plane OH bending vibrations and Al-O vibrations.

In addition, Fig. 2 shows FTIR absorption bands at approximately 3400cm^{-1} in the IR spectra of $qAl_{5.5}$, $qAl_{7.5}$, qAl_9, $qAl_{5.5(60°C)}$, $qAl_{7.5(60°C)}$, and $qAl_{9(60°C}$ (Fig. 2) associated with stretching vibrations of Al–OH groups and inter-layered water, which indicate that OH groups are tetrahedrally coordinated with Al^{+3} ions in gibbsite [2][12]. However, as observed in the spectra (Fig. 2), the cusp of the absorption bands broadens (decreasing% transmittance) with reducing pH. Moreover, the intensity of the absorption bands varies, where gibbsite samples synthesized at 60°exhibitrelatively lower % transmittance compared to their room temperature counterpart.

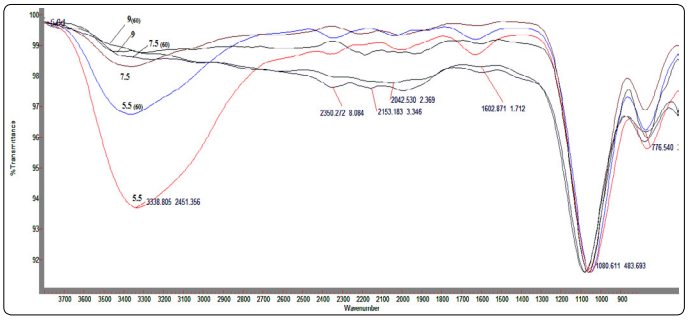

Fig 2. Overlapping FTIR spectra of the different synthesized gibbsite

Raman analysis of gibbsite coated quartz

Raman measurements in the range of 50-1250 cm^{-1} reveal distinct bands with frequencies and relative intensities. Regardless of the similarity in the character of the pure quartz

and gibbsite coated quartz substrates spectra, there exists a variation in the positions and intensity of the similarly shaped peaks for the two phases. The distinctive strong quartz peak of pure quartz substrates (q0) at 465cm^{-1} deviates slightly to 463cm^{-1} peak in the spectra of gibbsite coated quartz substrates (qAl) as shown in Fig. 3. The shift indicates tensile stress denoted by the slight broadening of the peak, invariably suggesting reduced crystallinity of the quartz. Other identified Raman shifts in the pure quartz include peaks at 352, 400 and 1137cm^{-1}. The variation in intensity points to the effect occlusion. The 465cm^{-1} peak of pure quartz grains show an intensity of 420 cm^{-1}, while that of quartz grains occluded with gibbsite are characterized by a relatively lower intensity. The decadence of the erstwhile prominent quartz peak indicates reduced crystallinity. In addition, quartz is observed to have a broad low-frequency Raman band at 199cm^{-1}, which is apparent in gibbsite coated quartz substrates. The broadness of this band has been attributed to the anharmonic coupling of an A1 phonon with a two-phonon (acoustic) mode [13].

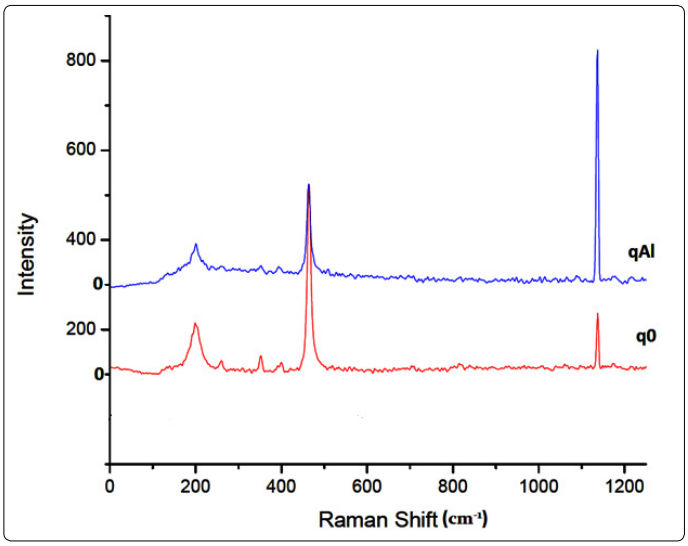

Fig 3. Raman spectra of pure quartz (q0) and gibbsite coated quartz (qAl)

Morphological characterization

The morphology of the gibbsite coated quartz was characterized using FESEM. Observation of samples synthesized at room temperature shows that the synthesized gibbsite is constituted by well-spaced clustered micrometer sized particles, (Fig. 4A) with no tendency to form aggregates. This property of not forming aggregates is directly related to the free-flowing characteristics of gibbsite. A second observed feature is the peculiar morphology of each particle, shown in higher magnification in Fig. 4B. Deep desiccation cracks occur after the growth of gibbsite, apparently attributed to the dehydration of the sample (Fig. 4C). The free-flowing precipitated gibbsite is depicted as lettuce shaped terminations [14] (Fig. 4D). Each particle is an agglomerate of platy crystals, with cubic terminations. It should be noted that the precipitated material coats the entire quartz substrate making the quartz surface indiscernible.

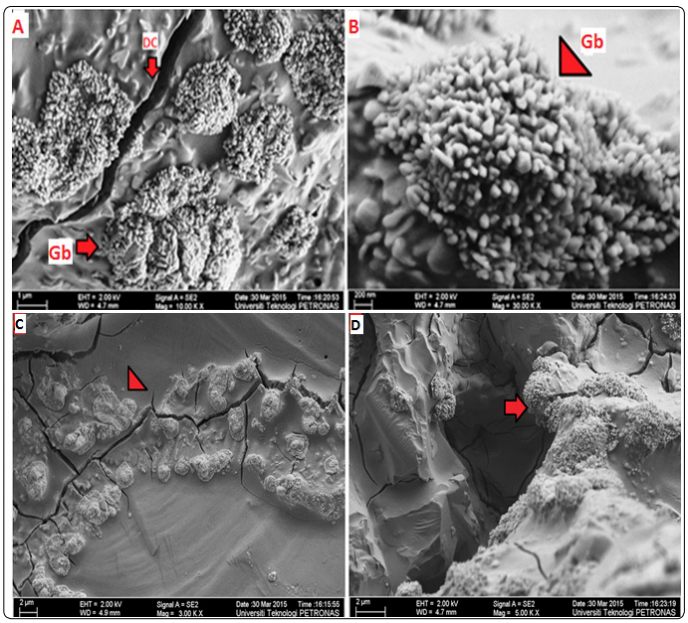

Fig 4. A) well separated clusters of synthesized gibbsite attributable to its free-flowing characteristic (G) B) distinct lettuce shape: infilling of gouges and notches on the quartz surface with agglomerated gibbsite clusters C) desiccation cracks D) gibbsite terminations on quartz edges

The samples synthesized at 60°C were also characterized. The morphology shows protuberances a top the quartz grains. The initially dispersed quartz grains become cemented by the crystallized gibbsite (Fig. 5A). A closer view (Fig. 5B) shows the quartz grains agglomerated by gibbsite. Fig. 5C shows the appearance of deeper and more prominent desiccation cracks on the gibbsite cement caused by the intensive dehydration process. At 60°C, the initial distinct lettuce shaped gibbsite crystals are transformed into well-defined hexagonal gibbsite crystal growths and prismatic laths as long as 3µm, as shown in Fig. 5D. The gibbsite prismatic crystals are arranged in overlapping layers.

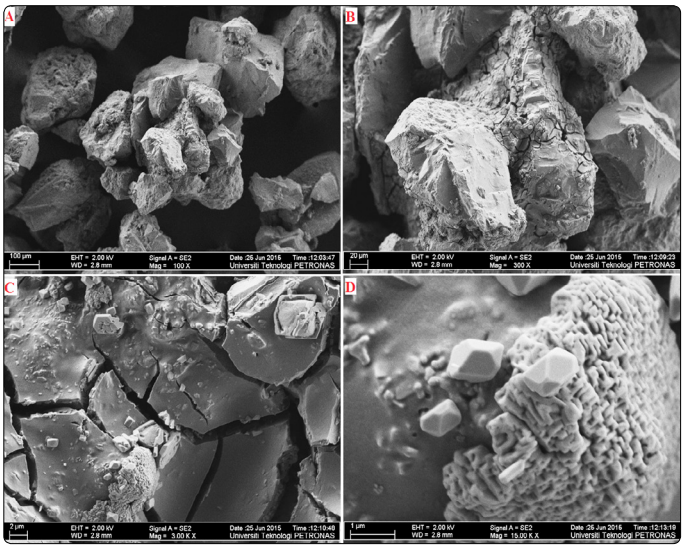

Fig 5. FESEM micrographs showing A) agglomerations of quartz grains B)cementation of quartz by gibbsite C) deeper and more prominent desiccation cracks D) highly crystallized polygonal gibbsite gibbsite crystals

The sample with the highest dissolved silica ($qAl_{9(60°C)}$) was further characterized, as shown in Fig. 6. The dissolved silica is

leached over the synthesized gibbsite. This makes the gibbsite crystals inconspicuous.

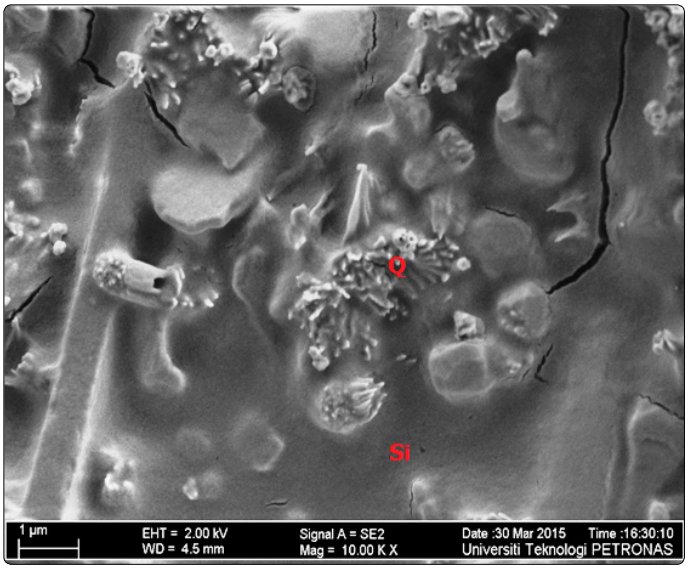

Fig 6. FESEM micrograph of $qAl_{9(60°C}$

Discussion

Effect of pH and temperature

$AlCl_3$ was hydrolyzed on quartz substrates to form insoluble colloidal and stable suspensions of aluminum oxides confirmed by the FTIR. The pH of the mother liquor controls the structure of the aluminum hydroxide precipitate. The variation in pH with time can be explained by the following mechanism. The trivalent compound [Aluminium chloride] basically hydrolyzes in water solution and ionizes to aluminium and chloride ions; whilst the water ionizes to hydrogen and hydroxide ions as illustrated by Eqs. (1) and (2); making the solution strongly acidic. The compounds are denoted with the subscript 'M'. Afterwards, the aluminium ions partially combines with the hydroxide ions released from the dissociation of water to form aluminium hydroxide (Eq.3), a compound which is only slightly soluble and precipitates from solution as a whitish solid. This process is catalyzed by heating up the solution and adding a base.

$MCl_3^- \rightleftharpoons M^{3+} + 3Cl$..... eqn (1)

$H_2O \rightleftharpoons H^+ + OH^-$ ....eqn (2)

$M^{3+} + 3OH^- \rightleftharpoons M(OH)_3$.....eqn (3)

As a base is added to the $AlCl_3$ solutions, the OH^- ions are deplete and neutralize the available H^+ ions to form water, causing the pH value to rise until the pH of the base being added is attained. The further addition of a base has little effect, with the pH remaining relatively constant based on the excess amount of OH^- in the system. Within this range, OH^- becomes constantly absorbed of by Al cations overtime to form oxy-hydroxide species. Thus, the OH^- ions are neutralized by the trivalent and H^+ ions, leading to the decline in pH. However, the pH of the null sample (pure quartz) remain constant at 12.5 possibly due to the absence of neutralizing agents.

The FESEM micrographs showed that gibbsite can be synthesized in the pH range selected for this study. This suggests gibbsite can be synthesized as long as there are available OH^- ions to hydrolyze $AlCl_3$. At room temperature, the synthesized gibbsites are basically lettuce shaped terminations. However, for stock solutions stored at a higher temperature (60°C), the gibbsite becomes more crystallized with well-defined polygonal structure. Thus, it can be inferred that the synthesis of gibbsite at 60°Cenhances its crystallinity without deforming crystal structure. This is consistent with the FTIR and Raman analyses, where the hydroxyl bands of samples stored at room temperature (25°C) exhibited lower %transmittance, due to water molecules locked in their crystal structure, compared to those synthesized at 60°C.

Quartz reactivity with Gibbsite

The bulk of quartz is composed of Si-O-Si [siloxane bonds] linkages, although the surface terminations consist of hydrophilic hydroxyl groups [terminal OH] [15], since the low-coordinated metal cations at the quartz surface are able to undergo hydrolysis in the presence of the water molecules to produce hydroxide layers (surface hydroxyls: -Si-OH) [16], as shown in Eq. (3). These hydroxide sites are very reactive, in that a proton from the adjacent solutions may be accepted or removed from the mineral surface, i.e. the silica surfaces can interact with water in two competing processes: physiochemical adsorption by hydrogen bonding (protonation) and chemical dissolution [17] expressed in Eqs. (4) and (5), respectively.

$H_2O + \equiv Si\text{-}O\text{-}Si \rightarrow 2\equiv Si\text{-}OH$.....eqn (3)

$\equiv Si\text{-}OH + H^+ \leftrightarrow \equiv Si\text{-}OH_2^+$.....eqn (4)

$\equiv Si\text{-}OH + OH^- \leftrightarrow Si\text{-}O^- + H_2O$.....eqn (5)

The adsorption process causes the oxygen of the water molecule to form a H-bond with the hydrogen of the OH surface group [OH coordinated to single silicon: Si-OH] as shown below in Fig. 7, based on proposed ab initio calculations [18]. Conversely, the water molecules are able to interact with the surface to cleave the Si-O-Si linkages [siloxane], resulting in hydrolyzed products [SiO^-], where a proton can be lost from the surface OH (deprotonation), usually in a basic solution [19][20][21]. Therefore, quartz dissolution is dependent on the hydrolysis of surface complexes. Theoretically, the presence of trivalent ions like Al^{3+} on quartz dissolution presents a different scenario. This study hypothesizes that the formation of Al complexes ($Al(OH)_3$) on the quartz surface, where the trivalent cations adsorb to SiO^- ligands to form new cationic ligands capable of stabilizing the quartz surface by combining with the surface Si- OH^- and dangling $OH^-$to form Al silicates and Al hydroxides, as depicted in Fig. 7.Although quartz is a non-reactive surface, it can serve as a media for gibbsite synthesis. The competing processes of chemical leaching and interfacial dissolution-reprecipitation between different materials are shown, where gibbsite is less distinct in solutions containing high dissolved silica ($q\ Al_{5.5(60°C)}$). Al hydr (oxides) coat the quartz surface and creates a surficial secondary layer that can allow the adsorption and agglomeration of other minerals.

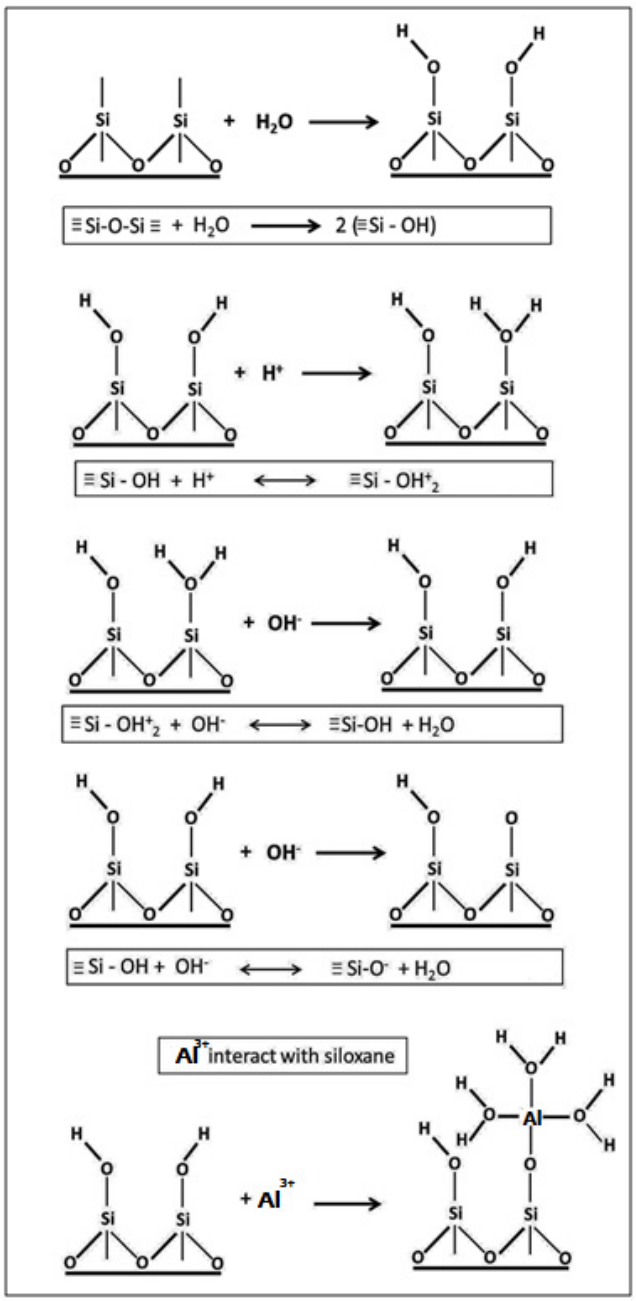

Figure 7. Model of quartz dissolution and Al^{3+} interaction with quartz

Synthesis of gibbsite

As shown in the FESEM images, gibbsite is a more efficient coating and cementing material at high temperature, which has been attributed to the increased planar form of Al hydroxide particles [22]. Thus, Al oxides will be efficient at reducing swelling and dispersion of clay as well as initiate a greater flocculent effect in a high temperature system, thereby improving soil hydraulic conductivity and tensile strength as suggested in earlier studies [23] [24]. The distribution of gibbsite is dependent on rapid precipitation or hydrolysis of $AlCl_3$ or other Al bearing compounds, pH, as well as temperature. The formation of gibbsite can retard quartz dissolution or resilication to a more stable kaolinite under a given H_4SiO_4 activity, while intense leaching at high temperatures in the presence of dissolved silica (H_4SiO_4) activity may enhance the formation of more stable clay minerals (kaolinite and smectite).

For industrial gibbsite precipitation, the product specified particle size distribution and morphology can be achieved by controlling the pH and temperature of gibbsite agglomeration and growth processes. At the microscopic level, both gibbsite agglomeration and growth occur on the crystal surface. This paper provides valuable insights into the growth mechanisms of gibbsite on quartz, which have direct influence on the particle growth pathways and reaction kinetics. Taking advantage of this new insight may bring about improvements in the crystallization technology of gibbsite, which is presently a sluggish process that requires trains of massive stirred tanks [9]. Thus, optimum conditions for synthesizing gibbsites in the presence of quartz include near neutral pH solutions at approximately 5.5 and temperature of 60ºC, i.e.$qAl_{5.5(60°C)}$.

Conclusion

The competing processes of chemical leaching and dissolution-reprecipitation between aluminium hydr (oxides) and quartz are shown, where gibbsite is distinctly more crystallized at higher temperature and low silica system. Thus, dissolved silica inhibits the crystallization of gibbsite minerals. Nonetheless, the precipitated Al hydr (oxides) coats the quartz surface and creates a surficial secondary layer that can possibly allow adsorption and agglomeration of other compounds. Gibbsite was precipitated within the pH range of 5 to 9, suggesting gibbsite can be synthesized as long as there are available OH^- ions to hydrolyze $AlCl_3$ and other Al bearing compounds.

Acknowledgement

This work was supported by the Petroleum Research Fund awarded to E. Padmanabhan.

References

1. Mutakyahwa MKD, Ikingura JR, Mruma AH. Geology and geochemistry of bauxite deposits in Lushoto District, Usambara Mountains, Tanzania. *Journal of African Earth Sciences*. 2003; 36(4): 357-69. doi: 10.1016/S0899-5362(03)00042-3

2. Tchakoute HK, Rüscher CH, Djobo JNY, Kenne BBD, Njopwouo D. Influence of gibbsite and quartz in kaolin on the properties of metakaolin-based geopolymer cements. *Applied Clay Science*. 2015; 107: 188-194. doi: 10.1016/j.clay.2015.01.023

3. Vazquez FM. Formation of gibbsite in soils and saprolites of temperate-humid zones. *Clay Minerals*. 1981; 16(1): 43-52.

4. Funakawa S, Watanabe T, Kosaki T. Regional trends in the chemical and mineralogical properties of upland soils in humid Asia: With special reference to the WRB classification scheme. *Soil Science and Plant Nutrition*. 2008; 54(5): 751-60. doi: 10.1111/j.1747-0765.2008.00294.x

5. Huang PM, Wang MK, Kampf N, Schulze DG. Aluminum hydroxides. In 'Soil Mineralogy with Environmental Applications'. *Soil Science Society of America: Madison*. 2002.

6. Fu W, Vaughan J, Gillespie A. Effects of inorganic anions on the morphology of sodium oxalate crystallized from highly alkaline solutions. *Crystal Growth & Design*. 2014; 14 (4): 1972-80. doi: 10.1021/cg5000952

7. Fu W, Vaughan J, Gillespie A. Aspects of the mechanism of nucleation and intergrowth of gibbsite crystals on sodium oxalate surfaces in concentrated alkaline solutions. *Crystal Growth & Design*. 2015a; 15(1): 374-83. doi: 10.1021/cg501465v

8. Fu W, Vaughan J, Gillespie A. In situ AFM investigation of heterogeneous nucleation and growth of sodium oxalate on industrial gibbsite surfaces in concentrated alkaline solution. *Chemical Engineering Science*. 2015b; 126: 399-405. doi: 10.1016/j.ces.2014.12.057

9. Fu W, Vaughan J, Gillespie A. In situ AFM investigation of gibbsite growth in high ionic strength, highly alkaline, aqueous media. *Hydrometallurgy*. 2016; 161: 71-76. doi: 10.1016/j.hydromet.2016.01.030

10. Coston JA, Fuller CC, and Davis JA. Pb^{2+} and Zn^{2+} adsorption by a natural aluminum- and iron-bearing surface coating on an aquifer sand. *Geochimica et Cosmochimica Acta*. 1995; 59: 3535-47. doi: 10.1016/0016-7037(95)00231-N

11. Davis JA, Coston JA, Kent DB, Fuller CC. Application of the surface complexation concept to complex mineral assemblages. *Environmental Science & Technology*. 1998; 32(19): 2820-28. doi: 10.1021/es980312q

12. Schroeder PA. Infrared Spectroscopy in clay science: In CMS Workshop Lectures , Teaching Clay Science, edited by Rule, A and Guggenheim, S, (*The Clay Mineral Society,Aurora, Colorado*)2002; 11: 181-206.

13. Jayaraman A, Kourouklis GA, Espinosa G P Cooper AS, VanUitert LG. A high-pressure Raman study ofyttrium vanadate (YVO.) and the pressure-induced transition from the zircon-type to the scheelite-type structure. *Journal of Physics and Chemistry of Solids*. 1987; 48(8): 755-59. doi: 10.1016/0022-3697(87)90072-2

14. Pedro KK, Helena SS, Antonio C, Vieira C, Pérsio de SS. Structure, surface area and morphology of aluminas from thermal decomposition of Al (OH) $(CH_3COO)_2$ crystals. *Anais da Academia Brasileira de Ciências*. 2000; 72(4): 471-495. doi: 10.1590/S0001-37652000000400003

15. Nangia S, Garrison BJ. Reaction rates and dissolution mechanisms of quartz as a function of pH. *J. Phys. Chem.*2008; 112(10): 2027-33. doi: 10.1021/jp076243w

16. Degen A, Kosec M. Effect of pH and impurities on the surface charge of zinc oxide in aqueous solution. *Journal of the European Ceramic Society*. 2000; 20(6): 667-73. doi: 10.1016/S0955-2219(99)00203-4

17. Nangia S,Washton NM, Mueller KT, Kubicki, JD, Garrison B. Study of a family of 40 hydroxylated β-cristobalite surfaces using empirical potential energy functions. *J. Phys. Chem B. C*. 2007; 111: 5169-177. doi: 10.1021/jp0678608

18. Lasaga AC, Gibbs GV. *Ab ibitio* quantum mechanical calculations of surface reactions – A new era?. In Aquatic chemical studies, edited by W. Stumm (ed.), John Wiley and sons, New York. 1990a; 259-89.

19. Xiao Y, Lasaga AC. Ab initio quantum mechanical studies of the kinetics and mechanisms of quartz dissolution: OH catalysis. *Geochimica et Cosmochimica Acta*. 1996; 60(13): 2283-95. doi: 10.1016/0016-7037(96)00101-9

20. Pelmenschikov A, Strandh H, Pettersson LGM, Leszczynski J. Lattice resistance to hydrolysis of Si–O–Si bonds of silicate minerals: ab initio calculations of a single water attack onto the (001) and (111) β-cristobalite surfaces. *J. Phys. Chem B*. 2000; 104(24): 5779-783. doi: 10.1021/jp994097r

21. Criscenti LJ, Kubicki JD, Brantley SL. Silicate glass and mineral dissolution: calculated reaction paths and activation energies for hydrolysis of a Q3 Si by H_3O^+ using ab initio methods. *J. Phys. Chem A*. 2006; 110: 198-206. doi: 10.1021/jp044360a

22. El-Swaify SA, EmersonWW. Changes in the physical properties of soil clays due to precipitated aluminum and iron hydroxides: I. Swelling and aggregate stability after drying. *Soil Science Society of America, Proceedings*. 1975; 39: 1056-1063. doi: 10.2136/sssaj1975.03615995003900060016x

23. El-Rayah, HME, Rowell DL. The influence of iron and aluminium hydroxides on the swelling of Namontmorillonite and the permeability of a Na-soil. *European Journal of Soil Science*. 1973; 24(1): 137-144. doi: 10.1111/j.1365-2389.1973.tb00749.x

24. Goldberg S, Glaubig RA. Effect of saturating cation, pH and aluminum and iron oxides on the flocculation of kaolinite and montmorillonite. *Clays & Clay Minerals*. 1987; 35: 220-27.